Interfacing Cell-Based Assays in Environmental Scanning Electron Microscopy Using Dielectrophoresis

ARTICLE *in* ANALYTICAL CHEMISTRY · MARCH 2011

Impact Factor: 5.64 · DOI: 10.1021/ac2002142 · Source: PubMed

8 AUTHORS, INCLUDING:

Khashayar Khoshmanesh
RMIT University
98 PUBLICATIONS **1,140** CITATIONS
SEE PROFILE

Kourosh Kalantar-zadeh
RMIT University
405 PUBLICATIONS **7,642** CITATIONS
SEE PROFILE

Sara Baratchi
RMIT University
36 PUBLICATIONS **616** CITATIONS
SEE PROFILE

David E Williams
University of Auckland
338 PUBLICATIONS **7,504** CITATIONS
SEE PROFILE

analytical chemistry

TECHNICAL NOTE

pubs.acs.org/ac

Interfacing Cell-Based Assays in Environmental Scanning Electron Microscopy Using Dielectrophoresis

Khashayar Khoshmanesh,[*,†,‡] Jin Akagi,[†] Saeid Nahavandi,[‡] Kourosh Kalantar-zadeh,[§] Sara Baratchi,[⊥] David E. Williams,[†] Jonathan M. Cooper,[¶] and Donald Wlodkowic[*,†]

[†]Department of Chemistry and MacDiarmid Institute for Advanced Materials and Nanotechnology, University of Auckland, Auckland, New Zealand

[‡]Centre for Intelligent Systems Research, Deakin University, Waurn Ponds, Australia

[§]School of Electrical and Computer Engineering, RMIT University, Melbourne, Australia

[⊥]Department of Biochemistry and Molecular Biology, Monash University, Clayton, Australia

[¶]The Bioelectronics Research Centre, Department of Electronics and Electrical Engineering, University of Glasgow, Glasgow, United Kingdom

Supporting Information

ABSTRACT: Development of the dielectrophoretic (DEP) live cell trapping technology and its interfacing with the environmental scanning electron microscopy (ESEM) is described. DEP microelectrode arrays were fabricated on glass substrate using photolithography and lift-off. Chip-based arrays were applied for ESEM analysis of DEP-trapped human leukemic cells. This work provides proof-of-concept interfacing of the DEP cell retention and trapping technology with ESEM to provide a high-resolution analysis of individual nonadherent cells.

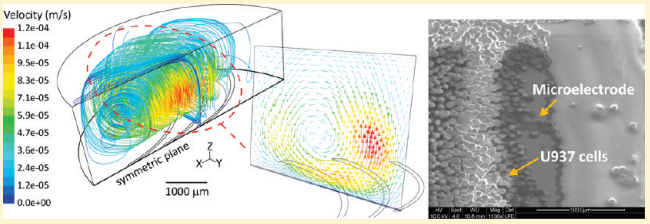

Live cell assays are currently an important part of drug discovery and personalized point-of-care diagnostics.[1] In this context, lab-on-a-chip (LOC) devices are being widely considered as emerging technologies that can support live cell analysis, enabling experimental measurement in parallel as well as multiparameter analysis at a single cell level.[2] They provide unique capabilities to monitor single-cell signaling dynamics, especially in rare subpopulations such as cancer or hematopoietic stem cells.[3,4]

Increasing numbers of microfabricated array-based technologies show innovative methods to position, register, and maintain single cells over extended periods of time. These among others include the use of droplet-based microfluidics, digital microfluidics, and microfluidic cell arrays.[5−8] Dielectrophoretic (DEP) technologies, exploiting the motion of polarizable particles in a spatially nonuniform electric field, have also been demonstrated for the selective mammalian cell trapping and analysis.[9−12]

Cell confinement under dielectrophoresis exploits the dipole moments that are induced in the cells upon exposure to electric field gradient. In this context, we have recently developed an innovative DEP cell immobilization technology for the dynamic analysis of drug-induced programmed cell death in hematopoietic tumor cells.[13] Our earlier study has provided a comprehensive mechanistic rationale for accelerated cell-based assays on DEP chips using real-time fluorescent cell labeling, making the dynamic analysis of investigational drugs in hematopoietic cancer cells feasible.[13]

Despite a large body of evidence using optical and electrical spectroscopies for the characterization of single living cells on a chip, no attempts have been so far made to interface microfabricated chip-based technologies with environmental scanning electron microscopy (ESEM). Conventional SEM requires high vacuum environments and biological samples must be, therefore, submitted to many preparative procedures to dehydrate and fix the sample.[14] This often introduces experimental artifacts and prevents imaging of living specimens. Conventional procedures often require a high level of technical competence and are time-consuming and hazardous.[14] The recent development and implementation of ESEM represents a new avenue for studies on biological specimens.

ESEM works in a vaporous atmosphere and thus facilitates imaging of biological samples without prior preparation such as desiccation and gold−palladium coating.[14] To retain single cells, however, both EM techniques involve laborious chemical surface modifications.[15,16] Only recently, we have reported application of the microfluidic cell arrays for hydrodynamic trapping of single hematopoietic tumor and stem cells.[3,4] These nonadherent cells are inherently very challenging to image due to immobilization difficulties and rapid dislodgement.

Received: January 25, 2011
Accepted: March 18, 2011
Published: March 28, 2011

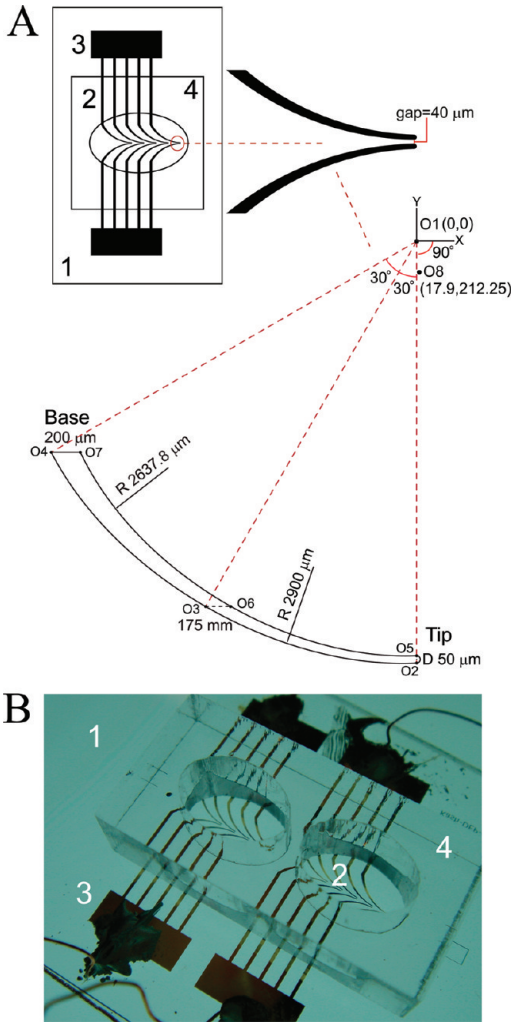

Figure 1. (A) Geometry of a DEP manifold with an array of chrome/gold microelectrodes deposited to a thickness of 500 Å/1500 Å on the glass substrate; (B) Assembled DEP device. Numbers on the schematics denote: 1, glass substrate; 2, microfabricated chrome/gold electrode array; 3, interconnecting pads providing AC signal actuation; and 4, PMMA/PDMS microculture chamber.

Here, for the first time, we show that chip-based DEP technology that can be successfully interfaced with ESEM imaging to provide a rapid and noninvasive cell immobilization of nonadherent cells under positive DEP (pDEP) force. Most importantly, nonadherent cells remain viable during processing and are well retained during imaging. Our innovative approach avoids extensive preparative procedures, is easy to perform for nonspecialized personnel, and thus, is prospectively amenable for automation. We propose that integration of DEP microchip technologies with SEM can considerably supplement conventional imaging and facilitate accelerated ESEM studies on nonadherent tumor cells.[3,4]

MATERIALS AND METHODS

DEP Chip Design and Fabrication. The DEP system took advantage of curved microelectrodes, obtained by intersecting two eccentric circles, as detailed in Supporting Information (Figure 1A). The microelectrodes have a width of 50 μm, a minimum gap of 40 μm along the centerline, and a distance of 1000 μm between the consequential pairs (Figure 1A). To fabricate microelectrode arrays, thin films of chrome/gold were deposited with a thickness of 500 Å/1500 Å on a glass substrate using an electron beam evaporation process and patterned using the standard photolithography techniques (Figure 1A).[13,17,18]

The DEP manifold consisted of a glass substrate that supports two independent sets of microelectrode arrays and a detachable poly(methylmethacrylate) (PMMA) microculture chamber with a height of approximately 2 mm (Figure 1B).[13]

Computational Analysis and Modeling. Microelectrode arrays were designed to support rapid cell immobilization at the regions of strong electric field formed between the opposite microelectrodes and generate weak electro-thermal vortices at the tips. Extensive simulations were performed to predict the performance of the DEP system. The simulations were performed using Gambit 2.3 software (Fluent, Lebanon, NH, USA) and the finite-volume based Fluent 6.3 software (Fluent, Lebanon, NH, USA), as given in the Supporting Information. Moreover, the polarization of cells upon exposure to the DEP field was predicted using the single-shell spherical model (Supporting Information).[13] The cells exhibited pDEP response under the selected combination of medium conductivity and frequency and were pushed toward the microelectrodes (Supporting Information). Due to symmetry, the governing equations were solved for three microelectrode pairs (Figure 2).

Cell Culture. Human histiocytic leukemia (U937) cells were obtained from ATCC (Manassas, VA, USA). All cell cultures were maintained in a complete RPMI1640 medium at 37 °C in a 5% CO_2 humidified atmosphere.[3,13,19] During experiments, cells were always in asynchronous and exponential phase of growth. Before DEP experiments, cells were washed three times with low electrical conductivity (LEC) buffer (8.5% w/v sucrose and 0.3% w/v dextrose) to decrease the electrical conductivity of the RPMI1640 medium from 2.5 ± 0.1 S/m down to 0.05 ± 0.005 S/m.[13,20] The electrical conductivity of the medium and buffer was measured using a conductivity meter (ECTestr11+, Eutech Instruments, Singapore).

Environmental Scanning Electron Microscopy (ESEM). Cells were exposed to the DEP field for 90−110 min (12 V_{p-p}, 20 MHz) in the LEC buffer.[13] Following cell immobilization, LEC buffer was gently aspirated and high resolution images were taken using an environmental scanning electron microscope (ESEM) operating under low vacuum mode according to the manufacturer's instructions (FEI Quanta 200 ESEM FEG, Hillsboro, OR, USA). The microscope has been equipped with a high performance thermal emission SEM column with dual-anode source emission geometry. The DEP chip was placed on a computer controlled Peltier cooled specimen stage. Resolution of ESEM has been adjusted at 4.0 nm using 10 kV acceleration and <100 Pa vacuum, enabling charge-free imaging and analysis of fully hydrated specimens. Development and optimization of the detailed protocol is discussed in more detail under the Results and Discussion section.

Data Analysis. Data analysis and presentation was performed using an open access ImageJ software suite (freely available at http://rsb.info.nih.gov/ij/webpage) and MeasureIT 5.1 (Olympus Soft Imaging Solutions GmbH). The Student's t test was applied for comparison between groups using SPSS 11 (Chicago, IL, USA) with significance set at $p < 0.05$.

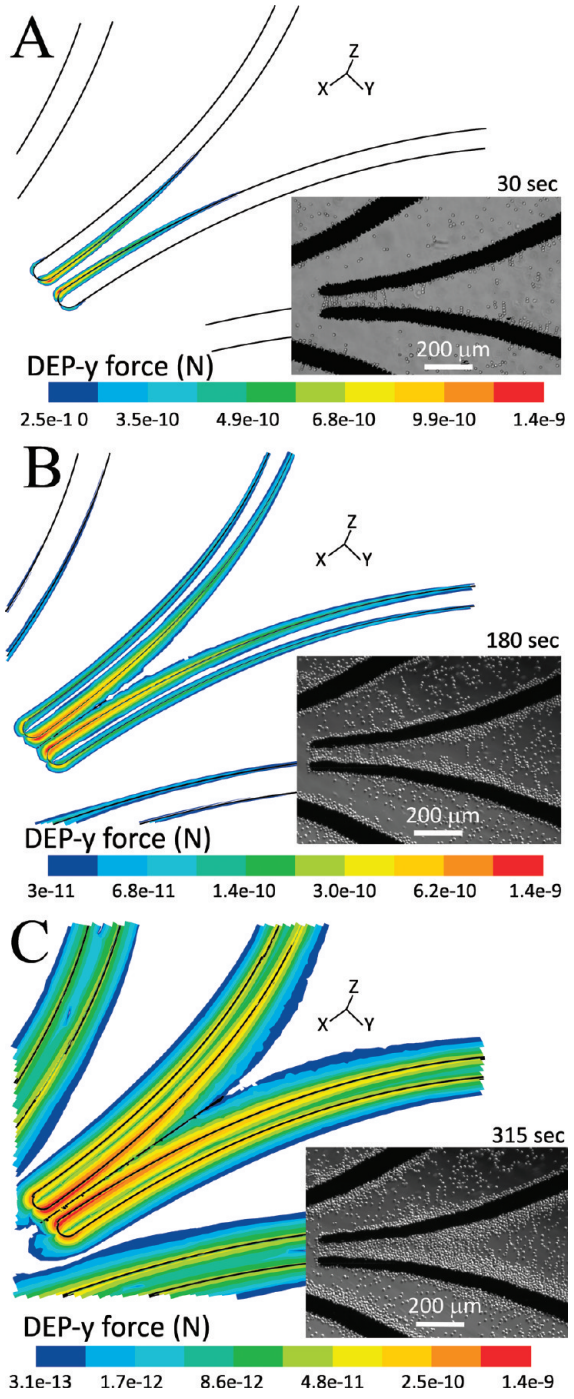

Figure 2. Dynamic analysis of cell accumulation and immobilization on a chip-based device. Computational modeling of the *y*-component of the DEP force at the bottom surface of the chamber and the immobilization of cells at different time intervals: (A) 30 s, (B) 180 s, and (C) 315 s after the activation of microelectrodes. Note that computational data are in good agreement (Pearson linear correlation $R^2 = 0.98$) with the actual accumulation of living U937 cells as shown in insets. Data represent a representative of three independent experiments performed in triplicate.

RESULTS AND DISCUSSION

Computational Modeling of DEP Responses. Assuming the geometry of U937 cells as homogeneous spherical particles, they experience a time-averaged DEP force described by the following equation:[21]

$$\overline{F}_{\mathrm{DEP}} = 2\pi r_{\mathrm{cell}}{}^3 \varepsilon_{\mathrm{medium}} \mathrm{Re}[f_{\mathrm{CM}}] \nabla E_{\mathrm{rms}}{}^2 \qquad (1)$$

where r_{cell} is the radius of the cell, $\varepsilon_{\mathrm{medium}}$ is the permittivity of the medium, E_{rms} is the root-mean-square value of the applied electric field, and $\mathrm{Re}[f_{\mathrm{CM}}]$ is the real part of the Clausius-Mossotti (CM) factor, representing the frequency-dependent polarization of cells under the DEP field. The $\mathrm{Re}[f_{\mathrm{CM}}]$ of human histocytic leukemia (U937) cells was modeled using the single-shell spherical model[22,23] (Supporting Information). The cells exhibited pDEP response with a $\mathrm{Re}[f_{\mathrm{CM}}] = 0.632$ under the selected combination of medium conductivity and frequency (0.05 S/m and 20 MHz) and were, therefore, attracted toward the microelectrodes.[13] Our models predicted that the attractive DEP force increases along the microelectrode structure until reaching a peak value at the tips. For example, the DEP force along the *y*-axis reaches a maximum value of 1.4×10^{-9} N at the tips (Figure 2). At the same time, the electro-thermal vortices circulated the medium within the chamber (Supporting Information).[13] The vortices acted like conveyor belts drifting cells from all around the chamber toward the microelectrodes where they were trapped under the pDEP force.

ESEM Analysis of DEP-Immobilized Human Leukemic Cells. In order to interface the DEP chip with the environmental scanning electron microscope (ESEM) and retain immobilized leukemic U937 cells in their positions between the microelectrodes, a novel protocol was established. A 100 μL aliquot of U937 cell suspension (approximately 1×10^3 cells) in a LEC buffer was injected to the PMMA microculture chamber (Figures 1 and 3A). We observed that the suboptimal quality of LEC buffers, which contain large amounts of the colloidal particles of sucrose and dextrose, can create a gelatinous cap that upon insertion into the ESEM chamber solidifies and reflects electrons away from the sample. This prevents obtaining SEM images from the cell sample. To rectify this problem, the LEC buffer was initially centrifuged at 3000 rpm (275*g*) for 5 min to remove any nondissolved particles and minimize accumulation of the colloidal residues on the surface of the cells and microelectrodes. The collected (purified) supernatant of LEC buffer was then used to wash and resuspend the cells while the conductivity of cell suspension was reduced to 0.05 S/m.

The cells were equilibrated for up to 2 min and then subjected to an AC signal of 12 $V_{p\text{-}p}$ at 20 MHz (Figure 3A).[13] Between 85−95% of cells in suspension were concentrated at the microelectrodes as opposed to only 1−5% of total population during random, gravitational sedimentation.[13] The cells were trapped between the microelectrodes within approximately 6 min, as described before.[13] The vortices played a crucial role in driving the suspended cells toward the microelectrodes. The vortices rotated within the chamber with their rotation axis parallel to the *x*-axis of the chamber and pushed the cells along the *y*-axis until being trapped at the microelectrodes (Supporting Information). Interestingly, the rate of cell immobilization can be correlated with the variations of DEP-*y* force at the bottom surface of the chamber. For example, 30 s after the activation of microelectrdoes, the cells were trapped only at the tip region, covering 3.2% of the shown area, where the DEP-*y* force varied from 2.5×10^{-10} to 1.4×10^{-9} N (Figure 2A). Accordingly, after 180 s, the cells were trapped along the microelectrode edges, covering 17.7% of the shown area, where the DEP-*y* force varied from

dx.doi.org/10.1021/ac2002142 |*Anal. Chem.* 2011, 83, 3217–3221

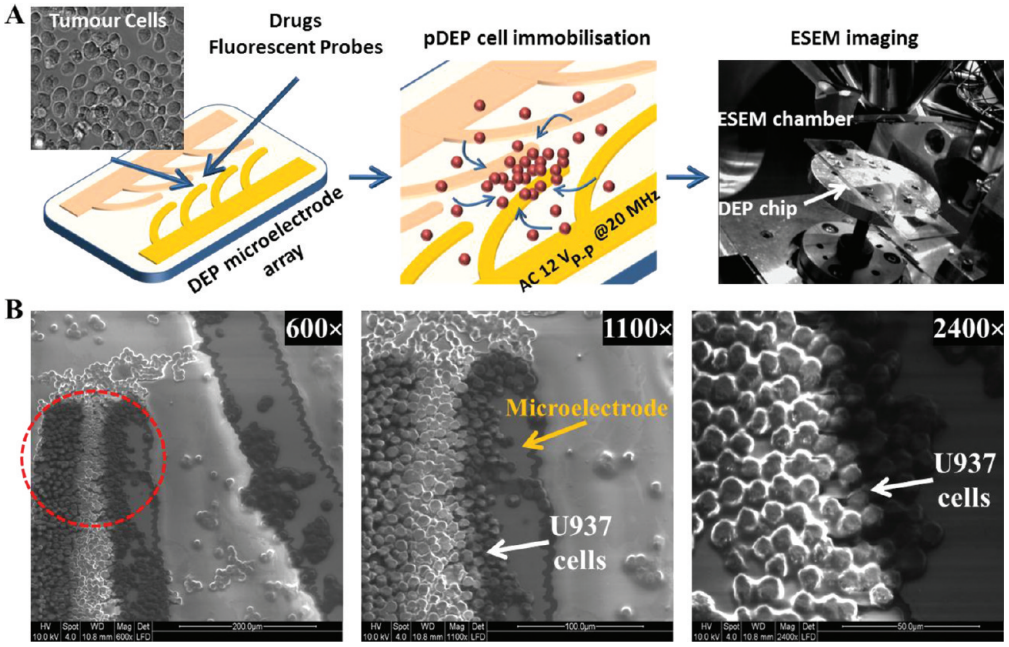

Figure 3. (A) Schematic showing the interface of the DEP microelectrode array chip with the scanning electron microscope. The complete procedure ranging from application of cell on a chip to high-resolution ESEM imaging can be performed within 90−110 min. (B) Human histiocytic leukemia cells trapped in a pDEP field are retained on the microelectrode array during the chip manipulation, transport, and ESEM imaging. After buffer aspiration. the microelectrodes were visualized in a low vacuum mode using FEI Quanta 200 ESEM. The high resolution imaging of the electrode tip with trapped U937 cells is shown (red circle).

3.1×10^{-11} to 1.4×10^{-9} N (Figure 2B). Finally, after 315 s, the cells covered the delta-shaped region between the microelectrdoes, covering 48.7% of the shown area, where the DEP-*y* force varied from 3.1×10^{-13} to 1.4×10^{-9} N (Figure 2C).

Following DEP cell immobilization, the LEC buffer inside the chamber was gently aspirated by manual pipetting. To minimize the cell dislodgment during buffer aspiration, the pipet tip was positioned only at the periphery of the microchamber and aspiration was slowly performed in 20 μL intervals. Reduction of the microchamber depth to 2 mm minimized the disturbance induced by pipet suction, improving the overall stability of the immobilized cells. Our data suggest that this is one of the most crucial steps as any excessive agitation or aspiration will result in cell dislodgment precluding successful imaging. In this context, control samples, i.e., following gravitational sedimentation of cells, exhibited nearly 100% dislodgement when a similar procedure was attempted. Morover, although a time period of 6 min was sufficient to immobilize the cells between the microelectrodes, some cells could still be dislodged during buffer aspiration. Our data indicated that extending the immobilization period up to 90 min overcomes this problem. To maintain the viability of cells during exposure to electric fields, the amplitude of AC signal can be safely reduced to 8 V_{p-p} after the initial 10 min without disturbing the stability of cells during buffer aspiration. As reported by us previously, the extended immobilization does not affect cell viability due to the very high frequencies.[13]

After buffer aspiration, the microelectrodes were de-energized and the chip containing an emulsion of the buffer was placed in a humidified atmosphere, transferred, and visualized in a low vacuum mode using FEI Quanta 200 ESEM (FEG, Hillsboro, OR, USA; Figure 3A). Panel 3B shows the high resolution SEM imaging of the microelectrode tip with immobilized leukemic U937 cells. Our data indicate that leukemic U937 were efficiency retained between the microelectrode arrays. Despite repeated manipulation, transportation and ESEM imaging dislodgement of cells from the arrays were not noticeable. Although to avoid excessive damage to cells, our imaging was performed at relatively low magnifications; the data provide proof-of-concept that DEP immobilization can be used to rapidly concentrate and trap hematopoietic tumor cells for ESEM imaging.

CONCLUSIONS

Conventional scanning electron microscopy has historically been restricted to material sciences and surface analysis. In contrast to conventional SEM, ESEM imaging is performed in a gaseous atmosphere under low vacuum mode.[14] These conditions greatly facilitate imaging of fully hydrated biological samples (deemed viable) without prior preparation such as desiccation and conductive coating with gold−palladium.[14,15] The main disadvantage of ESEM for cell biology is its less resolution and magnification than the transmission electron microscopy (TEM) or confocal microscopy.[14,15] It also mostly gives information about surface, shape modifications and plasma membrane specializations.[15,24] Because the SEM imaging is based on electron scattering at the surface rather than electron transmission, however, the analysis is fast and large amounts of samples can be analyzed with a much greater depth of view than in confocal imaging.[14] Such images provide a detailed 3D surface topographical information and yield more information than the flat or reconstructed images usually produced by confocal imaging. In addition, observations can be conducted with minimal specimen preparation, which is very attractive for studying interactions between mammalian cells and biomaterials that are, e.g., developed for tissue engineering.[14,25,26]

In conclusion, the DEP-based array, as described here, greatly reduces the complexity of conventional protocols and enables

high-resolution ESEM imaging on hematopoietic cells. Suspension cells such as hematopoietic tumor cells represent a particular challenge for both the conventional and SEM imaging.[3,4,6,27] Because they are nonadherent, their immobilization during processing and analysis is difficult and requires complex fixation protocols that can change the structure, morphology, and physical-chemical properties of the cells.[3,4] Only recently, we have reported application of the microfluidic cell arrays for hydrodynamic trapping and dynamic analysis of single hematopoietic tumor and stem cells over extended periods of time.[3,4] Enclosed microfluidic devices are, however, not suitable for interfacing with SEM. This work provides proof-of-concept interfacing of the open access dielectrophoretic (DEP) cell trapping with ESEM. We also discovered that, despite apparent advantages, many experimental microfabricated technologies are still relatively complex and often require a high level of technical competence to operate. Our work builds on the previously reported development of simplified DEP cell immobilization platform and presents its nothworthy extension for an ultrahigh-resolution analysis of individual nonadherent tumor cells.[13] Most importantly, as very low cell numbers and reagent volumes are required by DEP arrays, we envisage that single-cell ESEM imaging of clinically relevant subpopulations of rare cells will finally appear within the investigational reach.[9,28] We strongly envisage prospective applications of ESEM in the analysis of programmed cell death mode called apoptosis.[29] Despite subsequent introduction of numerous molecular assays, the morphological changes, detected by electron microscopy, still remain the "gold standard" to detect halmars of apoptosus such as profound surface alterations: smoothing, loss of microvillus structures, blebbing, shrinking of the plasma membrane, etc.[29,30] Although our current report concentrates on providing efficient DEP-based immobilization of hematopoietic cells for ESEM imaging, we currently continue the development of real-time ESEM imaging protocols that can provide 3D visualization of hematopoietic cells undergoing caspase-dependent apoptosis.

■ ASSOCIATED CONTENT

Supporting Information. Design specifications of DEP array (Supplementary 1), computational modeling the polarization spectra of human leukemic (U937) cells (Supplementary 2), and computational simulations of the DEP field (Supplementary 3). This material is available free of charge via the Internet at http://pubs.acs.org.

■ AUTHOR INFORMATION

Corresponding Author

*E-mail: khashayar.khoshmanesh@deakin.edu.au (K.K.); d.wlodkowic@auckland.ac.nz (D.W.).

■ ACKNOWLEDGMENT

Grant sponsors include the Endeavour Research Fellowships, Department of Education, Employment and Workplace Relations, Australia (K.K., S.B.); the Centre for Intelligent Systems Research, Deakin University, Australia (K.K.); Foundation for Research Science and Technology (FRST), New Zealand (D.W., J.A., D.E.W.); Faculty Research and Development Fund, University of Auckland, New Zealand (D.W., D.E.W.); MacDiarmid Institute for Advanced Materials and Nanotechnology (D.W., J.A., D.E.W.); and BBSRC, EPSRC, and Scottish Funding Council, United Kingdom, funded under the RASOR Program (J.M.C.).

■ REFERENCES

(1) Antczak, C.; Takagi, T.; Ramirez, C. N.; Radu, C.; Djaballah, H. *J. Biomol. Screening* **2009**, *14*, 956.
(2) Wlodkowic, D.; Cooper, J. M. *Anal. Bioanal. Chem.* **2010**, *398*, 193.
(3) Wlodkowic, D.; Faley, S.; Zagnoni, M.; Wikswo, J. P.; Cooper, J. M. *Anal. Chem.* **2009**, *81*, 5517.
(4) Faley, S. L.; Copland, M.; Wlodkowic, D.; Kolch, W.; Seale, K. T.; Wikswo, J. P.; Cooper, J. M. *Lab Chip* **2009**, *9*, 2659.
(5) Barbulovic-Nad, I.; Yang, H.; Park, P. S.; Wheeler, A. R. *Lab Chip* **2008**, *8*, 519.
(6) Di Carlo, D.; Wu, L. Y.; Lee, L. P. *Lab Chip* **2006**, *6*, 1445.
(7) Baret, J. C.; Beck, Y.; Billas-Massobrio, I.; Moras, D.; Griffiths, A. D. *Chem. Biol.* **2010**, *17*, 528.
(8) Brouzes, E.; Medkova, M.; Savenelli, N.; Marran, D.; Twardowski, M.; Hutchison, J. B.; Rothberg, J. M.; Link, D. R.; Perrimon, N.; Samuels, M. L. *Proc. Natl. Acad. Sci. U.S.A.* **2009**, *106*, 14195.
(9) Pethig, R. *Biomicrofluidics* **2010**, *4*, 022811.
(10) Pethig, R.; Talary, M. S. *IET Nanobiotechnol.* **2007**, *1*, 2.
(11) Thomas, R. S.; Morgan, H.; Green, N. G. *Lab Chip* **2009**, *9*, 1534.
(12) Voldman, J. *Annu. Rev. Biomed. Eng.* **2006**, *8*, 425.
(13) Khoshmanesh, K.; Akagi, J.; Nahavandi, S.; Skommer, J.; Baratchi, S.; Cooper, J. M.; Kalantar-Zadeh, K.; Williams, D. E.; Wlodkowic, D. *Anal. Chem.* **2011**, *86*, 2133.
(14) Muscariello, L.; Rosso, F.; Marino, G.; Giordano, A.; Barbarisi, M.; Cafiero, G.; Barbarisi, A. *J. Cell. Physiol.* **2005**, *205*, 328.
(15) Soligo, D.; Lambertenghi-Deliliers, G.; de Harven, E. *Scanning Microsc.* **1987**, *1*, 719.
(16) de Harven, E.; Soligo, D.; Lampen, N. *Scan Electron Microsc.* **1984**, 773.
(17) Khoshmanesh, K.; Zhang, C.; Tovar-Lopez, F. J.; Nahavandi, S.; Baratchi, S.; Kalantar-Zadeh, K.; Mitchell, A. *Electrophoresis* **2009**, *30*, 3707.
(18) Khoshmanesh, K.; Zhang, C.; Tovar-Lopez, F. J.; Nahavandi, S.; Baratchi, S.; Mitchell, A.; Kalantar-Zadeh, K. *Microfluid. Nanofluid.* **2010**, *9*, 411.
(19) Wlodkowic, D.; Skommer, J.; McGuinness, D.; Faley, S.; Kolch, W.; Darzynkiewicz, Z.; Cooper, J. M. *Anal. Chem.* **2009**, *81*, 6952.
(20) Huang, Y.; Wang, X. B.; Becker, F. F.; Gascoyne, P. R. *Biophys. J.* **1997**, *73*, 1118.
(21) Morgan, H. G. N. G. *AC Electrokinetics: colloids and nanoparticles*; Research Studies Press LTD: Baldock, 2003.
(22) Huang, H.; Holzel, R.; Pethig, R.; Wang, X. B. *Phys. Med. Biol.* **1992**, *37*, 1499.
(23) Irimajiri, A.; Hanai, T.; Inouye, A. *J. Theor. Biol.* **1979**, *78*, 251.
(24) Soligo, D.; de Harven, E. P.; Quirici, N.; Caneva, L.; Lambertenghi Deliliers, G. *Scanning Microsc.* **1995**, *9*, 175.
(25) Bell, E.; Merrill, C.; Lawrence, C. B. *Eur. J. Biochem.* **1972**, *29*, 444.
(26) McMenamin, P. G.; Wealthall, R. J.; Deverall, M.; Cooper, S. J.; Griffin, B. *Cell Tissue Res.* **2003**, *313*, 259.
(27) Yarmush, M. L.; King, K. R. *Annu. Rev. Biomed. Eng.* **2009**, *11*, 235.
(28) Stephens, M.; Talary, M. S.; Pethig, R.; Burnett, A. K.; Mills, K. I. *Bone Marrow Transplant* **1996**, *18*, 777.
(29) Wlodkowic, D.; Skommer, J.; Darzynkiewicz, Z. *Cytometry, Part A* **2010**, *77*, 591.
(30) Majno, G.; Joris, I. *Am. J. Pathol.* **1995**, *146*, 3.